Luminescence, absorption and excitation spectroscopy of $Cs_5Eu(N_3)_8$

1992 J. Phys.: Condens. Matter 4 2087

(http://iopscience.iop.org/0953-8984/4/8/022)

J. Phys.: Condens. Matter 4 (1992) 2087–2096. Printed in the UK

Luminescence, absorption and excitation spectroscopy of $Cs_5Eu(N_3)_8$

Karl Gatterer†, Colin D Flint‡, Harald P Fritzer† and Franz A Mautner†

† Institut für Physikalische und Theoretische Chemie, Technische Universität Graz, Rechbauerstrasse 12, A-8010 Graz, Austria

‡ Laser Laboratory, Department of Chemistry, Birkbeck College, University of London, Gordon House, 29 Gordon Square, London WC1H 0PP, UK

Received 10 October 1991, in final form 27 November 1991

Abstract. Electronic absorption, luminescence and laser excitation spectra of the complex ion $Eu(N_3)_8^{5-}$ in single crystals of $Cs_5Eu(N_3)_8$ have been measured at temperatures down to 4 K. Although the crystal structure shows the presence of only one type of $Eu(N_3)_8^{5-}$ complex ion, in which nearest N atoms form an approximate D_{4d} (square anti-prismatic) coordination polyhedron about the Eu atom, the spectra clearly show the presence of two distinct, but closely similar, types of Eu atoms. For one of these sites, emission from the $^5D_0$ state to all the expected crystal field states of the $^7F_J(J = 0–6)$ manifold and from the $^5D_1$ state to all of the $^7F_J(J = 0, 1, 2, 3)$ states is observed and, together with the absorption and the excitation spectra, permit the location of 56 of the 57 crystal field states expected below 23000 cm^{-1}.

1. Introduction

The synthesis, crystal and molecular structure of the title compound was recently reported [1] as one of a family of structurally similar lanthanide compounds. The crystals contain isolated $Eu(N_3)_8^{5-}$ complex ions with the nitrogen atoms nearest to the europium forming an approximately D_{4d} coordination polyhedron. This structure is of considerable interest. Firstly, crystals containing discrete eight-coordinate lanthanide ions with identical monodentate ligands are otherwise unknown [2]. Secondly, for D_{4d} symmetry an usually restrictive but controversial set of spectroscopic selection rules is applicable [3,4]. Thirdly, the azide ion is remarkable in possessing a high polarizability parallel to its axis with a much lower polarizability perpendicular to that axis, this being of special interest for the mechanism of hypersensitivity [5,6]. Fourthly, the absence of hydrogen atoms in the crystal suggested that the luminescence of the europium complex would have high quantum efficiency.

We have therefore initiated a study into the spectroscopic and energy transfer properties of the $Ln(N_3)_8^{5-}$ ion in suitable crystals. In this paper we report detailed electronic spectral data of $Cs_5Eu(N_3)_8$ at temperatures down to 4 K. We hope to deal with energy transfer and vibronic structure in related compounds in subsequent publications. The comparison with our studies on the cubic hexachloroelepasolites [7–9] is of interest.

0953-8984/92/082087+10$04.50

2. Structural data for $Cs_5Eu(N_3)_8$

At room temperature $Cs_5Eu(N_3)_8$ crystallizes [1] in the orthorhombic space group *Pbca* with a = 16.811(4) Å, b = 16.860(5) Å, c = 16.964(3) Å and Z = 8. There is no evidence from our differential scanning calorimetry or from precision magnetic measurements [10] of a phase transition in the temperature range 300–80 K, nor is there any indication of a phase transition in the range 300 K–4 K from the spectral measurements reported in this paper. Each europium atoms is surrounded by eight almost linear azide ions, all the azide ions are monodentate and non-bridging and the nearest Eu–Eu distances are about 9 Å. The eight $Eu(N_3)_8^{5-}$ complex ions in the unit cell are equivalent. The ligating atoms of the azide ions form an approximate D_{4d} coordination polyhedron about the europium atoms, although the crystallographic site symmetry of the europium is only C_2. Figure 1 shows the coordination polyhedron of the $Eu(N_3)_8^{5-}$ ion. We emphasize that the Eu–N=N=N angles are much closer to 90° than to 180°. The azide ligands are then almost tangential to the coordination sphere of the europium ion. This has important consequences for the observed spectra. A detailed description of the crystal and molecular structure is given in [1].

3. Experimental details

Large single crystals of $Cs_5Eu(N_3)_8$ were grown from aqueous hydrazoic acid as previously described [1]. **Caution:** hydrazoic acid and metal azides are potentially dangerously explosive, they should only be handled by personnel familiar with the hazards involved and in appropriately designed laboratories. These crystals have been prepared and handled (including gentle grinding) in our laboratories for several

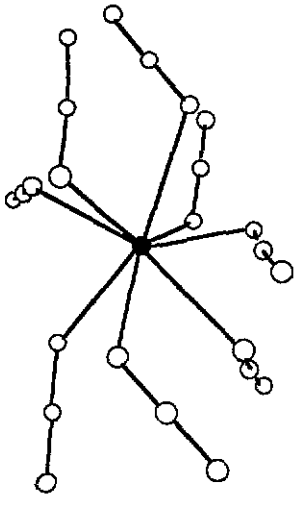

Figure 1. Molecular geometry of the $Eu(N_3)_8^{5-}$ ion in $Cs_5Eu(N_3)_8$. Key: ●, Eu; ○, N.

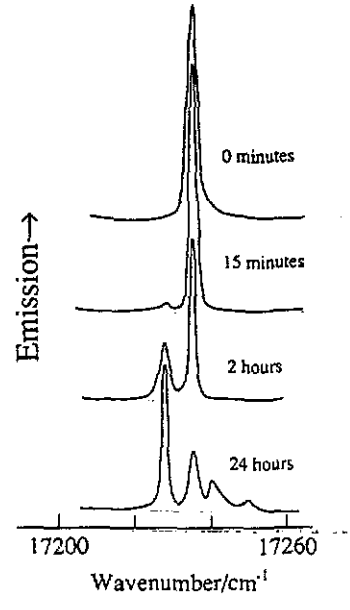

Figure 2. 465.8 nm excited 77 K luminescence spectra in $Cs_5Eu(N_3)_8$ following exposure to laboratory air for the stated times.

years without incident. The crystals are sensitive to atmospheric moisture and must be stored under dry nitrogen. The uptake of small quantities of water produces no visible change in the crystals, but causes additional absorption and emission bands to appear in the spectrum. The water may be conveniently detected by measuring the 465.8 nm excited 77 K luminescence spectrum in the region of the $^5D_0 \rightarrow {}^7F_0$ transition. With a special resolution of 2 cm^{-1}, good quality crystals show a single line at 17235 cm^{-1}, whilst even brief exposure to air results in the appearance of additional bands to both high and low energy (figure 2). The detailed spectral results in this paper were all obtained on crystals which gave luminescence spectra similar to figure 2 (0 min) both before and after the other measurements.

Single-crystal absorption spectra were measured between 17000 and 21500 cm^{-1} at temperatures from 300 to 30 K using a Bruins Instruments Omega 10 instrument fitted with a Leybold–Heraus closed cycle refrigerator. The spectral resolution achieved was about 5 cm^{-1} and several hundred scans were accumulated to give a high signal to noise ratio even on weak transitions. Luminescence spectra were measured using a 1 m monochromator fitted with a 1200 g mm^{-1} ruled grating, a cooled C31034A photomultiplier with photon counting detection and excitation from the 465.8 nm line of a 164-03 Spectra-Physics argon ion laser. The sample was maintained either in a simple 77 K cryostat or an Oxford Instruments CF100 flow cryostat. The special resolution was 2 cm^{-1} except for the weakest features of the $^5D_0 \rightarrow {}^7F_5$ and $^5D_0 \rightarrow {}^7F_6$ transitions where it was about 5 cm^{-1}. Excitation spectra were measured using a doubled or tripled Nd:YAG laser (Spectron Laser) pumping a Spectron Laser dye laser filled with coumarin 500 (18000–20500 cm^{-1}) or rhodamine 6G (17000–17500 cm^{-1}). The line width of this system is about 0.1 cm^{-1}. The emitted radiation was detected at 16275 cm^{-1} using a 0.25 m monochromator, cooled C31034A photomultiplier and EG&G boxcar integrator with a 10^{-3} s gate width opening 10^{-5} s after the laser pulse. All excitation spectral measurements (which we use in this study to provide high-sensitivity, high-resolution absorption spectra) were carried out at 4 K using a CF100 flow cryostat.

4. Results

4.1. Absorption and excitation spectra

Figure 3 shows the 30 K absorption spectrum of $Cs_5Eu(N_3)_8$ in the region of the $^7F_0 \rightarrow {}^5D_J (J = 0, 1, 2)$ transitions. At higher temperatures additional hot bands due to transitions from the thermally populated components of the $^7F_1$ state may be detected. Study of the temperature dependence of the spectra and comparison with the luminescence spectra shows that all the relatively sharp, stronger features are due to electronic origins. Under the moderate resolution of these absorption experiments not all components of the $^7F_1$ and $^5D_J (J = 0, 1, 2)$ states expected in the C_2 site symmetry can be resolved but the observed number of bands is equal to that expected in quadrate symmetry. The broad complex structure to high energy of the $^7F_0 \rightarrow {}^5D_2$ transition is vibronic in origin. At higher wavenumber (not shown) the absorption spectrum is dominated by a very much stronger and broader band centred at 27400 cm^{-1} which we assign as being primarily ligand to metal charge transfer in character. The $4f^6 \rightarrow 4f^5 5d$ transitions of Eu^{3+} in complexes of other ligands are generally at very much higher energy than this in absorption [11]. Using the 'optical electronegativity' values for N_3^- and Eu^{3+} of $\chi(N_3^-) = 2.8$ and $\chi(Eu^{3+}) = 1.9$ [12]

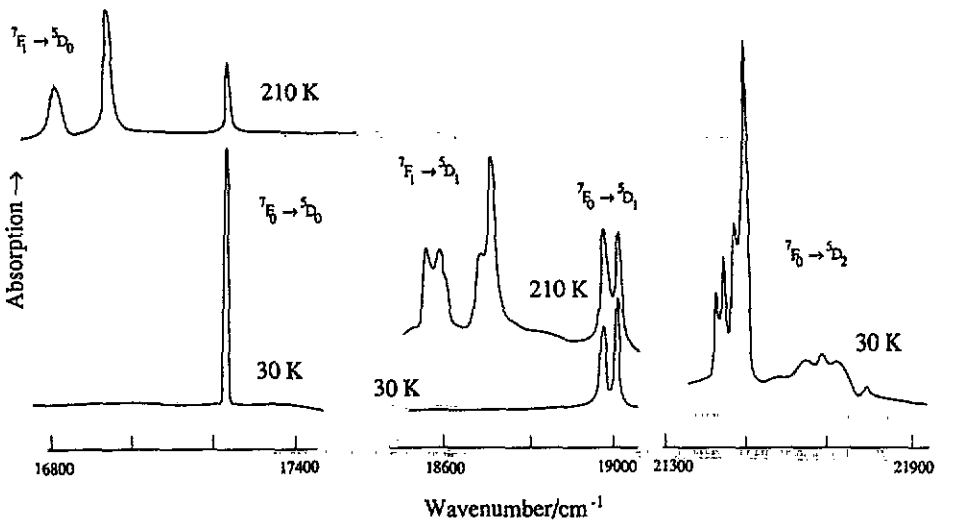

Figure 3. Single-crystal absorption spectra of $Cs_5Eu(N_3)_8$ in the 16 800–21 900 region at the stated temperatures.

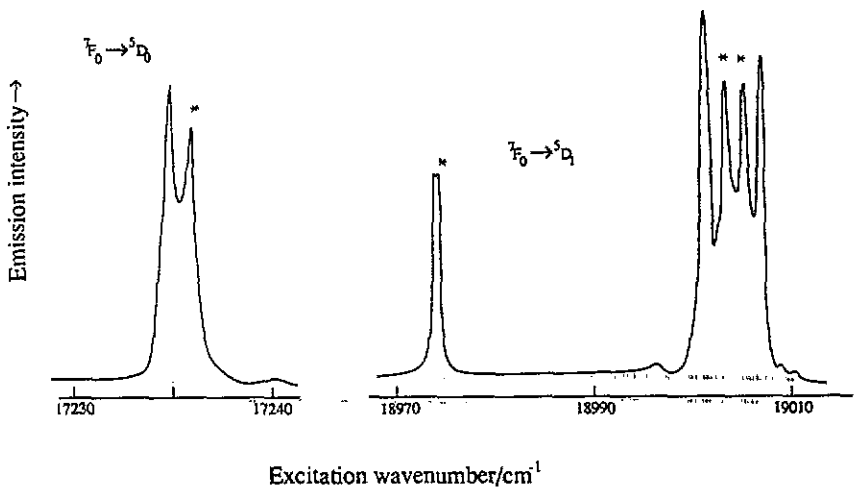

Figure 4. 10 K dye laser excitation spectra of $Cs_5Eu(N_3)_8$ single crystals in the region of the $^7F_0 \rightarrow {}^5D_0$, $^5D_1$ transitions; observation wavenumber 16 287 ± 20 cm^{-1}. Note the different linear dispersion of the spectra in the two regions.

we estimate (following [12]) that the charge transfer $N_3^- \rightarrow Eu^{3+}$ absorption band should occur at about 27 000 cm^{-1} in excellent agreement with this assignment.

Figure 4 shows the high-resolution excitation spectra recorded in the regions of the $^7F_0 \rightarrow {}^5D_0$ and $^5D_1$ absorption bands. In each case the bands detected in absorption are split into two components separated by 1–2 cm^{-1}. This splitting clearly shows the presence of two very similar but non-identical sites in the crystal which are not evident from the crystal structure. The large Eu–Eu distances and the small dipole strengths mean that interionic couplings can be eliminated as the source of this splitting. These

sites are termed I and II, bands attributed to transitions on site II are indicated by asterisks in figure 4 and subsequent figures, although the assignments to specific sites are only evident from careful consideration of the luminescence spectra. For each site the splitting of a $J = 1$ level into a closely spaced doublet and a well separated singlet is consistent with the approximately D_{4d} coordination sphere and the C_2 site symmetry of the complex ion. Attempts to selectively excite the two sites were not successful, presumably due to energy transfer between them. At much high sensitivity the electronic origins are seen to be accompanied by extensive vibronic structure which we hope to consider in a later paper.

4.2. Luminescence spectra

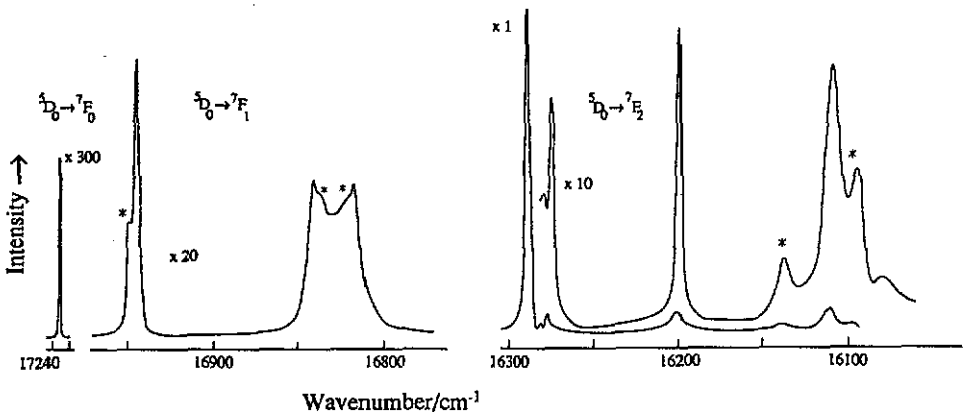

Figure 5. 465.9 nm excited 77 K luminescence spectra of $Cs_5Eu(N_3)_8$ in the regions of the $^5D_0 \rightarrow {}^7F_0$, $^7F_1$, $^7F_2$ transitions. Note the ordinate expansion factors.

Figure 5 shows the moderate resolution luminescence spectrum of $Cs_5Eu(N_3)_8$ at 77 K in regions of the $^5D_0 \rightarrow {}^7F_J (J = 0\text{–}2)$ transitions. The emission is remarkably intense and the quantum efficiency must be high. The $^5D_0 \rightarrow {}^7F_0$ transition has been discussed in section 3. The splitting pattern for the $^7F_1$ state into a singlet and a more closely spaced doublet exactly parallels that observed in the $^5D_1$ state although the splittings are about four times greater in approximate agreement with the factor calculated by Judd [13]. There seems no reason to require different radial functions for f electrons with parallel and anti-parallel spin as in other lattices [13]. The same pattern occurs for both site I and site II, and the wavenumbers of corresponding transitions are closely similar on the two sites. However, the emission intensities from each of the components of the $^5D_0 \rightarrow {}^7F_1$ transition on site I are several times weaker than those from site I even though the $^7F_0 \rightarrow {}^5D_0$ and $^7F_0 \rightarrow {}^5D_1$ components on the two sites have comparable transition moments in the absorption. The $^5D_0 \rightarrow {}^7F_2$ region is dominated by one very intense transition at high wavenumber with at least six other weaker bands. Clearly some of these must occur on site II and the wavenumbers of the $^7F_2$ levels must be significantly different on the two sites. Further information on these assignments may be derived from the $^5D_1 \rightarrow {}^7F_J (J = 1, 2)$ transition, figure 6, since in this case several of the transitions occur at detectably different wavenumbers on the two sites. In this way a consistent set of energy levels for the five components of the $^7F_2$ state may be derived for site I and at least three of the components of this state for site II are identified. Only

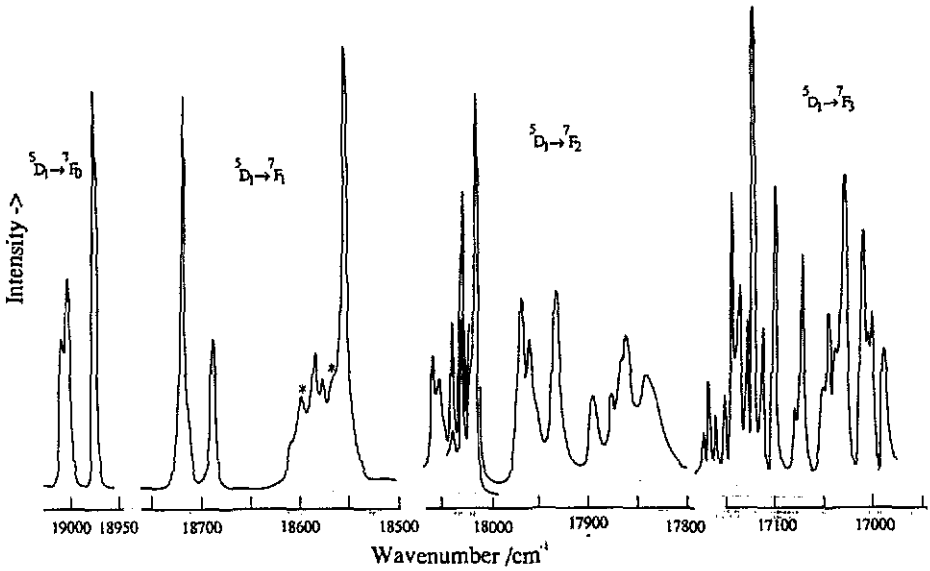

Figure 6. 465.8 nm excited 77 K luminescence spectra of $Cs_5Eu(N_3)_8$ in the regions of the $^5D_1 \rightarrow {}^7F_0$, $^7F_1$, $^7F_2$, $^7F_3$ transitions.

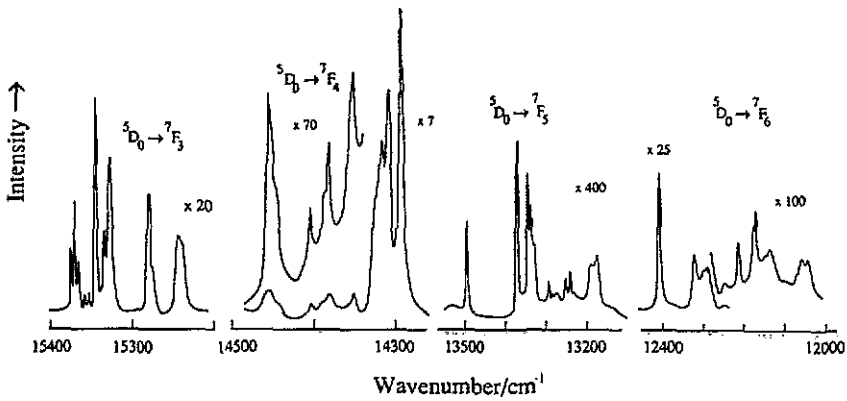

Figure 7. 465.8 nm excited 77 K luminescence spectra of $Cs_5Eu(N_3)_8$ in the regions of the $^5D_0 \rightarrow {}^7F_3$, $^7F_4$, $^7F_5$, $^7F_6$ transitions. Note the ordinate expansion factors.

one weak transition at 17 875 cm^{-1} is not assigned in this analysis, it may be vibronic based on the very much more intense origins to high energy.

The two transitions $^5D_1 \rightarrow {}^7F_3$ (figure 6) and $^5D_0 \rightarrow {}^7F_3$ (figure 7) show 23 and 12 lines respectively and transitions from both sites must be involved. The simplest way to assign the $^5D_1 \rightarrow {}^7F_3$ transitions belonging to site I is to seek triplets of lines separated by 27 cm^{-1} and 6 cm^{-1} corresponding to the excited state splitting. In this way 18 of the lines may be tentatively assigned although several involve two overlapping transitions. This provides tentative energies for all seven components of the $^7F_3$ state. These tentative assignments are then confirmed since the same set of seven levels can account for seven of the stronger features of the $^5D_0 \rightarrow {}^7F_3$ transition. The remaining features in both spectra can then be consistently assigned

to site II, five of the expected seven components being located. As before, the transitions at site II are generally weaker than those at site I, and whilst the crystal field patterns are somewhat similar, they are not identical.

The only observed transitions involving the ^7F_J (J = 4–6) are those originating from the $^5D_0$ levels and it is therefore impossible to distinguish transitions occuring on the two sites from the measurements we have carried out. In the absence of any other information we assume that the most intense transitions originate from site I and the few remaining lines are left unassigned but probably arise from site II. The barycentres of the J = 4, 5 and 6 manifolds are then consistent with those observed for other Eu^{3+} compounds.

The derived energy levels from absorption, emission and excitation spectra are collected in table 1. A detailed table of assignments of individual lines is available from the authors.

5. Discussion

5.1. Nature of sites I and II

The absorption and excitation spectra suggests that two closely similar Eu^{3+} sites exist in comparable numbers in each of several crystals. This is inconsistent with the published crystal structure. We presume that the x-ray method is unable to detect the tiny differences between the sites, presenting a statistical average [14]. The difference might arise from the conformation of the coordinated azide ions or from the presence of another species in the lattice. Since the spectra are very sensitive to the uptake of moisture by the crystals and the original preparation is not under anhydrous conditions it is possible that the Z = 8 unit cell might contain one or more water molecules. These would be analytically undetectable in a strongly hygroscopic material with a large unit cell mass.

The lower intensity of the emission from the second site but comparable dipole strength in absorption is consistent with the perturbation of the second site by a nearby water molecule since the high frequency and strongly polar O–H vibration is known to relax the $^5D_0$ and $^5D_1$ levels of Eu^{3+} efficiently [15]. A similar explanation has been given for the optical and energy transfer properties of $Cs_2NaEuCl_6$ although in that case the number of perturbed sites is small [9].

We note that whilst the detailed crystal field splitting of the LSJ terms at the two sites are distinguishable, the barycentres are similar suggesting almost identical coordination polyhedra at the two sites.

5.2. Crystal field terms

The first coordination sphere of the Eu^{3+} approximates to D_{4d} symmetry, we take this point group as the starting point for the analysis of the energy levels. In particular the splittings of the two J = 1 levels are consistent with the existence of an approximate fourfold rotation axis at the Eu^{3+} site. Blasse has pointed out that the D_{4d} point group is 'very peculiar' in that the $^5D_0 \rightarrow {}^7F_2$ transition is electric-dipole forbidden, and quotes examples such as $EuW_{10}O_{36}^{9-}$ where the magnetic dipole $^5D_0 \rightarrow {}^7F_1$ transition dominates the $^5D_0 \rightarrow {}^7F_2$ transition leading to an overall orange luminescence [3]. Other examples have been discussed by Thompson and Kuo [16].

Table 1. Wavenumbers, $\nu(cm^{-1})$, of the crystal field levels of the $Eu(N_3)_8^{5-}$ ion in $Cs_5Eu(N_3)_8$ determined by luminescence spectroscopy at 77 K unless otherwise indicated.

LSJ term	Site I	Site II	*LSJ* term	Site I	Site II
$^7F_0$	0	0			
$^7F_1$	288	285			
	401	407		4825	
	422	417		4931	
				4945	
	948			4987	
	955		$^7F_6$	5021	
$^7F_2$	960	967		5061	
	1042	1110		5094	
	1140	1159		5099	
				5133	
	1864	1860		5161	
	1868	1877		5173	
	1890	1882		5191	
$^7F_3$	1901				
	1907				
	1955	1961			
	1992	1998			
	2780		$^5D_0$	17235	17236[a]
	2787				
	2830			18974	18974[a]
	2854		$^5D_1$	19001	19003[a]
$^7F_4$	2882			19007	19005[a]
	2908				
	2918			21427[b]	
	2926			21445[b]	
	2942		$^5D_2$	21468[b]	
				21492[b]	
	3738				
	3860				
	3887				
	3894				
	3898				
$^7F_5$	3906				
	3939				
	3979				
	3992				
	4044				
	4058				

[a] Measured at 10 K by dye laser excitation spectroscopy.
[b] Measured at 30 K by single-crystal absorption spectroscopy.

The $Eu(N_3)_8^{5-}$ ion is quite different in that one component of the $^5D_0 \rightarrow {}^7F_2$ transition is more than five times stronger than any other transition and even some of the weaker features of the $^5D_0 \rightarrow {}^7F_2$ transition are stronger than the strongest component of the $^5D_0 \rightarrow {}^7F_1$ transition. The emission appears bright red. The remarkable difference between the luminescence of the $Eu(N_3)_8^{5-}$ ion and all other ions with D_{4d} coordination geometry probably arises from high polarizability (and polarizability anisotropy) of the azide ligand which enormously enhances the hypersensitive $^5D_0 \rightarrow {}^7F_2$ transition which acquires electric dipole intensity due to the C_2

site symmetry. In this case the specific geometry of the ion may play an important role. The arrangement of the azide ligands is such that angular displacements of f-electron density due to the electronic transition will substantially perturb the azide electron density due to the high polarizability of the azide ion parallel to its molecular axis. Radial displacements of f-electron density will have much less effect since they are coupled to the perpendicular azide polarizability. The $^5D_0 \rightarrow {}^7F_4$ transition (which is also electric-quadrupole allowed, and therefore subject to hypersensitivity) is also several times more intense than the $^5D_0 \rightarrow {}^7F_1$ transition.

Table 2. Decomposition of relevant angular momentum eigenfunctions to D_{4d}.

J value	D_{4d} representations
0	A_1
1	$A_2 + E_3$
2	$A_1 + E_2 + E_3$
3	$A_2 + E_1 + E_2 + E_3$
4	$A_1 + B_1 + B_2 + E_1 + E_2 + E_3$
5	$A_2 + B_1 + B_2 + 2E_1 + E_2 + E_3$
6	$A_1 + B_1 + B_2 + 2E_1 + 2E_2 + E_3$

The D_{4d} point group presents a number of problems in notation and axis conventions which have lead to inconsistent correlations to R_3 and hence incorrect selection rules [3,4]. We consider the problem in detail elsewhere [10]. Using the character tables of Atkins *et al* [17], with the xz and yz planes defined so as to contain only the Eu atom, we find the decomposition of the spherical symmetry J states given in table 2. The allowed electric dipole transitions are then $A_1 \rightarrow B_2, E_1$, $A_2 \rightarrow B_1, E_1$ and $E_3 \rightarrow B_1, B_2, E_1, E_2$; whilst $A_1 \rightarrow A_2, E_3$, $A_2 \rightarrow A_1, E_3$ and $E_3 \rightarrow A_1, A_2, E_2, E_3$ are magnetic-dipole allowed.

Whilst the splitting of the $J = 1$ levels implies near fourfold symmetry, there is no obvious correlation for the $J \geqslant 2$ levels. In this case it seems that the splitting pattern is not determined by the nearest neighbour environment. Again we suspect that the role of the polarizability anisotropy may be significant. The ligand polarization contribution to the static crystal field will add significantly to the usual nearest neighbour 'point charge' electrostatic contribution in determining the crystal field parameters. The dynamic ligand polarization will dominate the intensity of the hypersensitive transitions and any transitions which mix significantly with them. The result is that the C_2 molecular symmetry dominates the splitting patterns and intensity distributions rather than the nearest neighbour D_{4d} symmetry. A calculation aimed at testing some of these ideas is planned.

Acknowledgments

We thank the British Council for a travel grant to KG during which the spectroscopic measurements were made, and the Birkbeck College Research Committee for an equipment grant (to CDF). The manuscript was prepared during visits by CDF to Graz and by HPF to Birkbeck College financed in part by the Technische Universität Graz. We thank Dr Marco Bettinelli (Universitá di Padova) for helpful discussions.

References

[1] Mautner F A and Krischner H 1990 *Monat. Chem.* **121** 781
[2] Sinha S P 1976 *Struct. Bonding* **25** 69
[3] Blasse G 1988 *Inorg. Chim. Acta* **142** 153
[4] Fritzer H P and Gatterer K 1992 unpublished
[5] Mason S F 1975 *Mol. Phys.* **30** 1829
[6] Mason S F and Stewart B 1985 *Mol. Phys.* **55** 611
[7] Bettinelli M and Flint C D 1990 *Chem. Phys. Lett.* **167** 45
[8] Bettinelli M and Flint C D 1991 *J. Phys.: Condens. Matter* **3** 4433
[9] Bettinelli M and Flint C D 1991 *J. Phys.: Condens. Matter* **3** 7053
[10] Fritzer H P and Gatterer K 1992 unpublished
[11] Blasse G 1976 *Struct. Bonding* **26** 43
[12] Jørgensen C K in Lippard S J (ed) 1970 *Prog. Inorg. Chem.* **12** 101
[13] Judd B R 1977 *Phys. Rev. Lett.* **39** 242
[14] Bunzli J-C G and Pradervand G-O 1987 *J. Chem. Phys.* **85** 2489
[15] Horrocks W De W and Albin M 1984 *Prog. Inorg. Chem.* **31** 1
[16] Thompson L C and Kuo S C 1988 *Inorg. Chimica Acta* **149** 305
[17] Atkins P W, Child M S and Phillips C S G 1984 *Tables for Group Theory* (Oxford: Oxford University Press)